NLR-TP-2005-514

Improvement and verification of low-speed aerodynamic characteristics of a supersonic civil transport aircraft

J. van Muijden

Approved by:

Author	Reviewer	Managing department
16-09-2005	mL 16/05	16/9
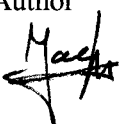
Summary

For supersonic civil transport aircraft, the low-speed aerodynamic characteristics form an important factor in its operational capabilities and in its economic viability. Low drag is a prerequisite to meet the present and future noise and emissions requirements. Innovative concepts for leading-edge devices aiming at the improvement of low-speed aerodynamic efficiency are investigated. From computational analysis of a series of leading-edge flap designs, the two most promising devices are selected for experimental verification, viz. a double-hinge leading-edge flap and a deep-hinge leading edge flap design. In the course of comparing experimental and computational results, discrepancies are observed that are satisfactorily dealt with by adding the wind tunnel struts and the strut-wing connections in the computational analysis. Reynolds number extrapolations from wind tunnel scale to full-scale are obtained using CFD. It is concluded that the design approach based on CFD has significantly contributed to the success of configuration development, meeting the target efficiency improvement. Furthermore, the influences of geometrical details that differ in the design phase and the validation phase have been assessed.

Contents

(22 pages in total)

List of symbols and abbreviations

b	Wing span
c	Wing chord
C_D	Drag coefficient
C_d	Local drag coefficient
C_L	Lift coefficient
C_l	Local lift coefficient
C_M	Pitching moment coefficient
C_P	Pressure coefficient
M	Mach number
Re	Reynolds number
x	Streamwise coordinate
y	Spanwise coordinate

α	Angle-of-attack
Δ	Increment
η	Relative span position, 2y/b

DNW	German-Dutch Wind Tunnels Organisation
EARSM	Explicit Algebraic Reynolds Stress Model
ENFLOW	Euler/Navier-Stokes Flow simulation system
EPISTLE	European Project for the Improvement of Supersonic Transport Low-speed Efficiency
EUROSUP	European project on Supersonic aircraft aerodynamic technology improvement
F1	Low-speed wind tunnel of ONERA, located in Fauga
GARTEUR	Group for Aeronautical Research and Technology in Europe
HST	High-speed wind tunnel of DNW, located in Amsterdam
NaS	Navier-Stokes
SST	Supersonic wind tunnel of DNW, located in Amsterdam

This page is intentionally left blank.

1 Introduction

For supersonic civil transport aircraft and supersonic business jets currently under consideration, low-speed aerodynamic efficiency is an essential factor in the operational capabilities and in the economic viability of such aircraft. Stringent present and future noise and emission requirements need to be respected by new types of aircraft. For supersonic transport aircraft, anticipating the regulations of the future implies the necessity to take a major step in technological progress of controlling the low-speed aerodynamic flow over typical high-speed wing shapes. The approach is basically aiming at minimisation and control of the amount of flow separation and vortex formation over the wing, thereby reducing drag.

In this paper, innovative leading-edge device concepts for a supersonic civil transport to improve low-speed aerodynamic efficiency are investigated. The basic shape of the configuration that is used for the leading-edge device studies has been designed within the framework of the European research project EUROSUP [1], running in the period 1996-1998. In this project, the design objectives focussed on the three speed regimes; supersonic (Mach 2), transonic (Mach 0.95, see e.g. [2]) and low-speed flow (Mach 0.25). In order to come up with a configuration that fulfils the aerodynamic efficiency requirements for each speed regime, the best design approach appeared to be a supersonic optimisation to obtain the basic wing shape, and optimisation of leading and trailing edge flap deflections to meet the requirements in the transonic and low-speed regimes. At the end of the project it became clear that design and analysis methodologies have matured to a sufficient level for supersonic and transonic flow, whereas at low-speed conditions it was much more difficult to meet the a priori given requirements. This is in part due to the existence of separated flow at the design point. The flaws in low-speed analysis capabilities have been addressed in a follow-up effort, initially in a GARTEUR action group during 1999, and later on in the European research project EPISTLE [3], an acronym for "European Project for the Improvement of Supersonic Transport Low-speed Efficiency", running from 2000 to 2003. The EPISTLE project focussed on investigating parameter variations of different types of leading-edge flaps, assessing their sensitivities and working towards a feasible design methodology. As a side effect of this approach, highly promising devices were identified and improved to the point of meeting the requirements for low-speed aerodynamic efficiency. Current interest in vortical flow control over a double-delta type wing is also reflected in [4].

In the following, the selection of most promising devices and the validation of their operational capabilities with wind tunnel data is described. Furthermore, the integrated application of CFD-methods during and after the wind tunnel tests for the determination of the impact of wind tunnel model support struts on measured balance data is described. Finally, CFD is used in a Reynolds number extrapolation in order to obtain performance data at full-scale flight conditions.

2 Double-hinge leading-edge flap evolution

Part of the work performed by NLR consisted of investigating the possible benefits of a so-called double-hinge leading-edge flap. The datum geometry, stemming from the EUROSUP project, has a single-hinge leading-edge flap with limited flap chord and three spanwise flap segments, although the design specifications allow for as many as five spanwise flap segments. This indicates the possibility to subdivide two of the spanwise flap segments into smaller ones. Each flap segment has its own optimised flap deflections. At the design lift coefficient, however, the datum configuration shows a vast amount of separated flow. Improvement of the aerodynamic efficiency of the configuration is sought in a reduction of flow separations. Within the EPISTLE project, the target value for the improvement in aerodynamic efficiency is set at 20 percent relative to the datum geometry.

Within the allowable limits for leading edge devices, the flap chord can be varied. In an initial attempt to define the double-hinge geometry, the aft hinge line has been selected at the most rearward position, thus maximising the allowable flap chord. The foremost hinge line has been selected at 50 percent between the leading edge and the aft hinge line. Initial deflections for each of the flap segments are obtained by taking the flap segment deflections of the datum, and applying half of its value to both front and aft flap per segment. Figure 1 shows the configuration and the spanwise segmented double-hinge flap concept.
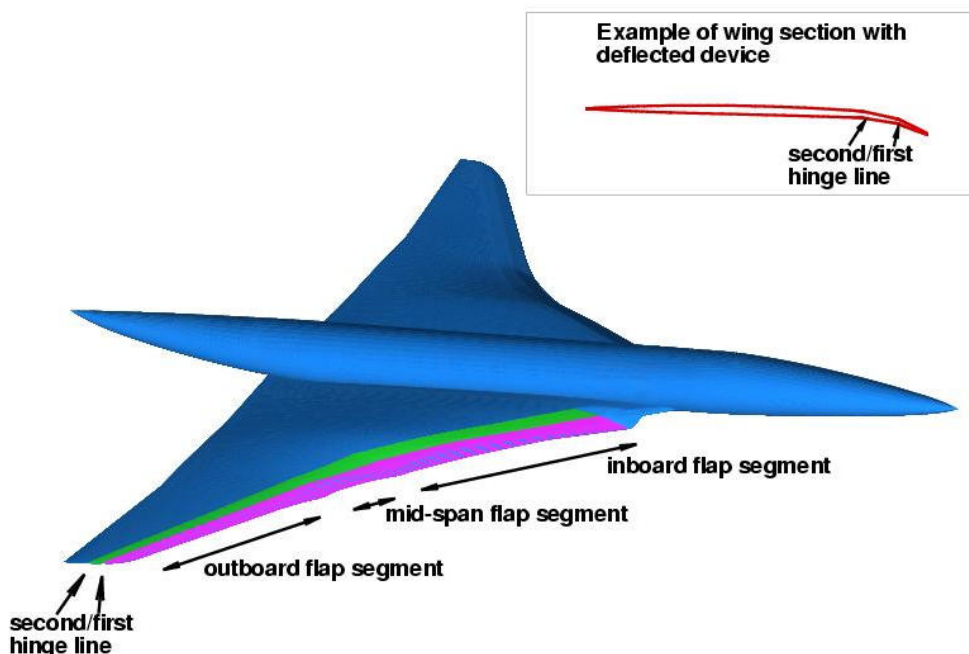
Figure 1 Low-speed configuration of supersonic civil transport with double-hinge leading-edge flap system

The analysis of this initial spanwise segmented double-hinge flap concept showed a remarkable step forward in aerodynamic efficiency. Motivated by this improvement, the flow solutions on the initial double-hinge configuration were analysed and it was decided that a further increase in deflection for each of the foremost flap segments could be beneficial in reducing the separated flow over the wing at the design point. The second double-hinge configuration indeed showed the expected improvement, but did not yet meet the target aerodynamic efficiency. The analysis loop was performed again with somewhat larger deflections applied to the foremost flap segments. The third and final double-hinge configuration again showed improvement in aerodynamic efficiency, this time meeting the target value. As an illustration of this evolutionary process, the total pressure losses at a span position of 75 per cent for the datum and the three evolutionary double-hinge configurations are shown in Figure 2.
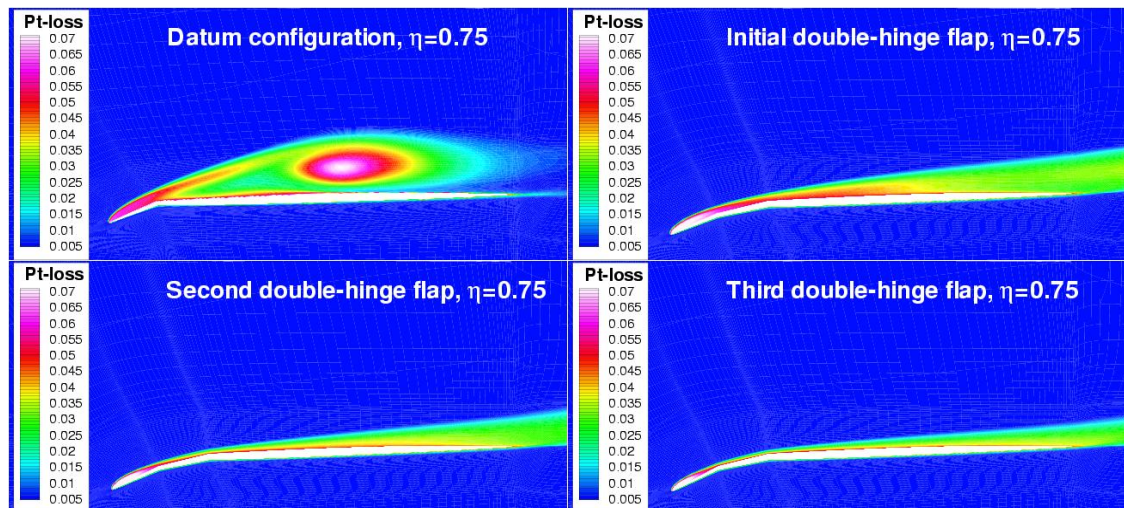
Figure 2 Evolution of separated flow at design lift on outer wing section by applying deflection variations of a double-hinge flap system, visualised by total pressure losses

It should be noted that the manual design process as described above implies that no full search through the available design space has been executed. Thus, other parameter combinations for the double-hinge leading-edge flap - in terms of flap chord, number and extent of spanwise flap segments, and flap deflections – may well exist with potentially higher aerodynamic efficiencies.

3   Selection of promising devices

During the parametric variation studies, many types of leading-edge devices have been studied, involving a vast range of design parameter values and partners working in parallel, using their own CFD-methods. The low-speed configuration developed in the EUROSUP project is taken as a reference, its aerodynamic efficiency value at design lift coefficient is normalised to unity. Figure 3 summarises all computational results for the leading-edge devices under consideration, including those for the double-hinge configurations as well as the clean supersonic wing shape without any leading-edge devices. All data are scaled with the reference value of the datum configuration, thus showing whether an improvement of efficiency is achieved. Despite the uncertainties involved in this comparison, caused by computational meshes of varying resolution, different flow solvers and a variety of turbulence models, devices featuring an aerodynamic efficiency exceeding the target value emerge. From all available types of leading-edge devices, the two most promising ones, viz. the third double-hinge configuration and the deep-hinge configuration (designed by DLR, deep-hinge referring to the underwing location of the apparent hinge line), were selected for validation in a wind tunnel test campaign.
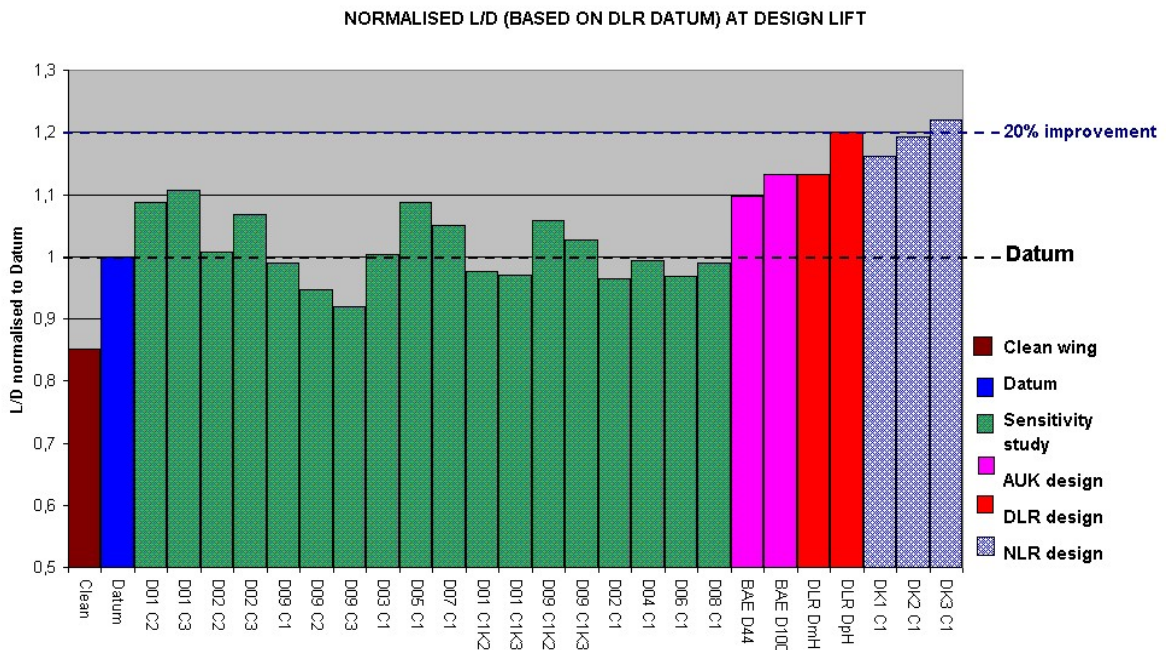
Figure 3 Relative merits of low-speed leading-edge flap system concepts for a future SCT at design lift

4   Wind tunnel model and test

Experimental data for the datum low-speed configuration on scale 1/80, obtained in the DNW-HST wind tunnel in Amsterdam, are available from the EUROSUP project, see e.g. [5]. This model consists of a sting-mounted fuselage with exchangeable wings representing the shapes for the three speed regimes at supersonic, transonic and low-speed conditions. The model scale has been chosen to facilitate testing of the same model in the supersonic wind tunnel DNW-SST. The low-speed configuration is shown in Figure 4. Additional experiments have been conducted at an early stage of the EPISTLE project, using the same model in the DNW-HST wind tunnel, in order to verify transition strip effectiveness and repeatability of pressure data, and to obtain additional oil flow visualisations of flow development. Also, the basic supersonic wing shape without leading edge flap deflections has been tested at low-speed conditions. For the sake of testing new leading-edge flap designs, however, a larger model was preferred in order to be able to manufacture the relatively small details of the flaps with higher accuracy, and to obtain experimental data at higher Reynolds numbers.

Figure 4 Scale 1/80 wind tunnel model of the low-speed datum configuration in the DNW-HST wind tunnel

A large model (scale 1/22) has been designed with interchangeable leading and trailing edges and a separate fuselage. Geometrical variations are limited only to the leading-edge parts of the wing, the remainder of the model has a fixed geometry. The flexibility in the wind tunnel model design approach may prove its value in the future, in case more and different flap types and flap settings need to be tested. Furthermore, the possibility exists to test different fuselage cross-sectional shapes if the current circular shape is deemed inadequate. The two selected innovative leading-edge devices have been manufactured separately. In addition, the datum leading-edge

flap has been manufactured as well in order to be able to verify the improvements in aerodynamic efficiency. The wind tunnel model has been designed by DLR. The manufacturing has been performed by the work shops of DLR, NLR and ONERA in a combined effort to allow for a timely availability of the model.

The wind tunnel tests on the large model have been performed in the ONERA F1-tunnel. The model is supported by three struts, see Figure 5 left. Although such model supports have been used before, this was the first test with the centreline strut in front of the wing struts, due to the very specific configuration at hand. For the connection of the struts to the comparatively thin wing, pylons have been used, see Figure 5 right. The shape and setting angle of the pylons have been determined on the basis of CFD-results, aiming at minimisation of disturbing influences at the low-speed design point. Experimental data from the tests comprise surface pressure data, balance data of forces and moments, wake surveys, and flow visualisations. In view of the usage of three struts, with balance measurements including forces on the exposed parts of the struts extending above the strut housing, it can be expected that corrections need to be applied to the experimental force and moment data.

Figure 5 Scale 1/22 wind tunnel model mounted on three struts (left) in the F1 wind tunnel, and details of the connection of wing struts to thin wing using streamline pylons (right)

5   Comparison of performance of leading-edge devices

It is emphasized that all CFD-methods used within the project have undergone an acceptance test in the early stages of the project using the 1/80-scale datum configuration DNW-HST wind tunnel data. Only CFD-methods that passed the test have been applied again in subsequent design and analysis work packages. In this way, it is assured that user experience, computational meshes and turbulence models have matured to the point where reliable predictions can be expected for this type of flow, which is containing large regions of separated flow at higher

incidences. The NLR ENFLOW CFD-system [6], using an explicit algebraic turbulence model based on the two-equation k-ω turbulence model [7], has passed the acceptance test, see [5, 8].

Before execution of the wind tunnel tests on the 1/22 scale model, predictions have been obtained by NLR for the selected innovative leading-edge devices. A comparison is made with the datum configuration in order to assess the flow development and resulting performance of the innovative devices. Current experience with these configurations, including leading-edge flap deflections and significant regions of separated flow, has led to meshes having over 4 million cells for accurate results. Comparison of the predicted lift curves is shown in Figure 6a. It is shown that over the main part of the incidence range, the lift of the new flaps is lower than that of the datum configuration. From the viewpoint of delaying separation onset, being one of the objectives of the innovative devices, this is a success. The lift curves are showing a significant delay of vortex lift development as compared to the datum configuration. Predicted drag polars are shown in Figure 6b. As expected, the new designs have lower drag than the datum configuration. At the design point, the drag of the innovative designs is approximately 60 drag counts below that of the datum configuration. The difference between the double-hinge and deep-hinge flap is however extremely small, both configurations exhibit practically the same lift and drag curves. In pitching moment behaviour, see Figure 6c, the differences are somewhat larger although the global trend is identical for all three configurations. The innovative devices show a deviation from each other after separation onset. Finally, the aerodynamic efficiencies (lift-to-drag ratios) are depicted in Figure 6d. Except at very low lift values, the curves of the new designs are very much identical and well above the datum. A disappointing fact, however, is that the current predictions at the design point do not match the earlier predictions, obtained during the double-hinge evolution analysis. The only obvious reason for this finding is found in non-negligible geometrical differences, which will be addressed in more detail below.
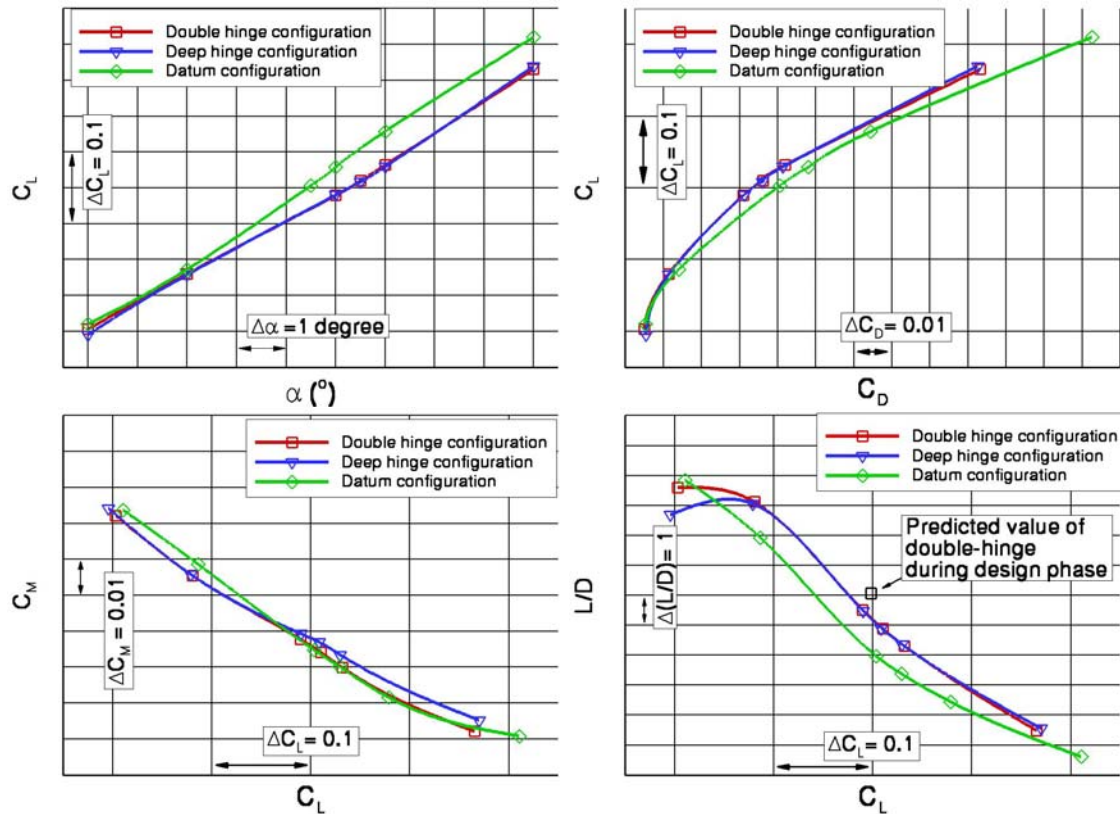
Figure 6 Comparison of predicted performance for three configurations at M=0.25 and Re=22.6 million; a) Top left: lift curve; b) Top right: drag polar; c) Bottom left: pitching moment curves; d) Bottom right: lift-to-drag ratio.

6   Reynolds number extrapolation

Extrapolation to full-scale has been performed using CFD. The comparison of results, using the same plot scales as for the low-Reynolds number case, is shown in Figures 7a-d. Results obtained at flight Reynolds number show very similar behaviour to those at wind tunnel Reynolds number. The drag is lower, which can almost completely be attributed to the friction drag reduction with the increase in Reynolds number. As a consequence, the aerodynamic efficiency is higher. However, even at flight Reynolds number, the current prediction of efficiency for the double-hinge configuration is still somewhat lower than the predicted lift-to-drag value at low Reynolds number during the design phase. In Figure 8a, a more detailed drag polar comparison is shown using the results at both Reynolds numbers. The drag at flight Reynolds number is, for all configurations, reduced as a natural consequence of friction drag reduction. However, it is more interesting to note that the drag reduction due to identical variations in Reynolds number is not the same for each configuration, see Figure 8b. Especially interesting is that for the double-hinge configuration, the drag reduction at design lift coefficient

is smaller than that for the deep-hinge configuration. This finding might be attributed to the appearance of two sharp suction peaks in the pressure distributions, resulting from the two sharp geometrical knuckles at the hinge line positions. The adverse pressure gradients involved in such sharp suction peaks are a source of boundary layer momentum loss. With increasing Reynolds number, the suction peaks tend to become higher, thereby increasing the boundary layer momentum losses. A minor but significant geometrical detail is suspected to play a role. In the double-hinge configuration, the geometry is actually changing slope in a discontinuous manner at the hinge lines. In the deep-hinge configuration, knuckle rounding at the hinge line has been applied from the start, which has a beneficial impact on suction peak pressure gradients, as will be shown later on. It is anticipated that knuckle rounding is beneficial for the flow development, in terms of decreasing the suction peak increase with increasing Reynolds number at the hinge positions and thereby reducing the viscous flow momentum losses.
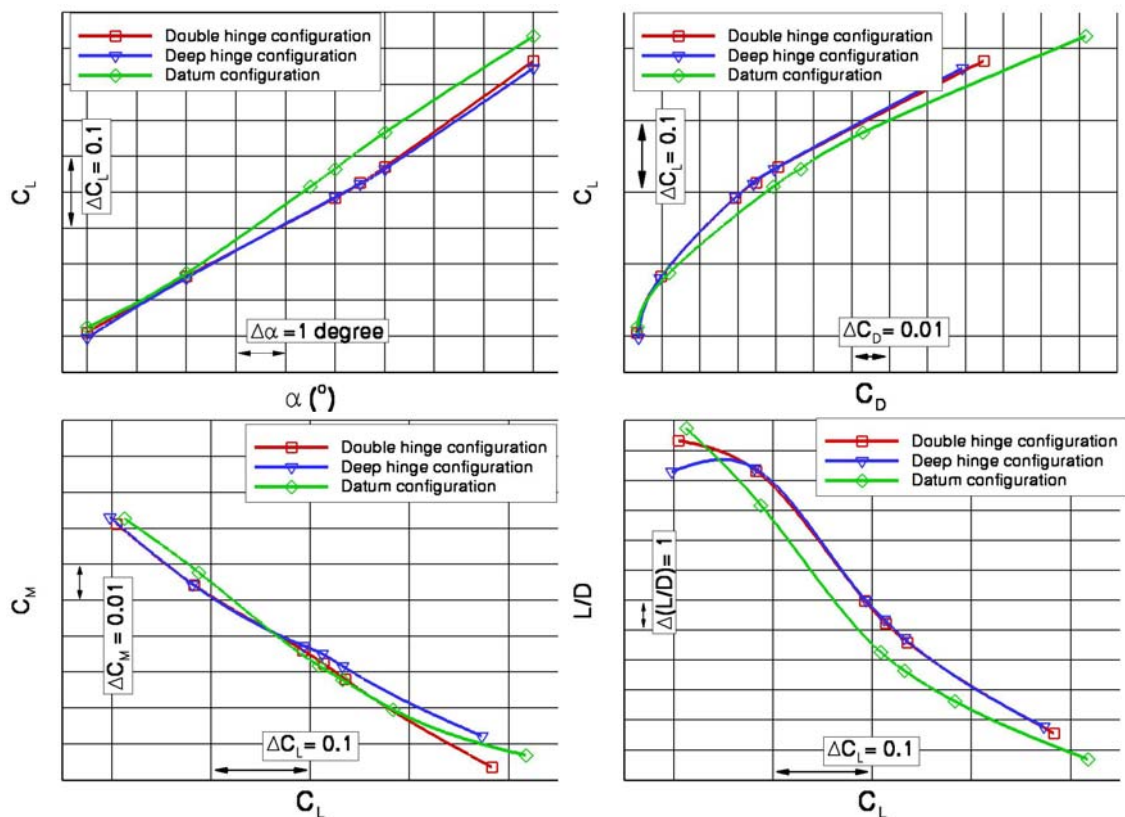
Figure 7 Comparison of predicted performance for three configurations at M=0.25 and Re=161 million; a) Top left: lift curve; b) Top right: drag polar; c) Bottom left: pitching moment curves; d) Bottom right: lift-to-drag ratio.
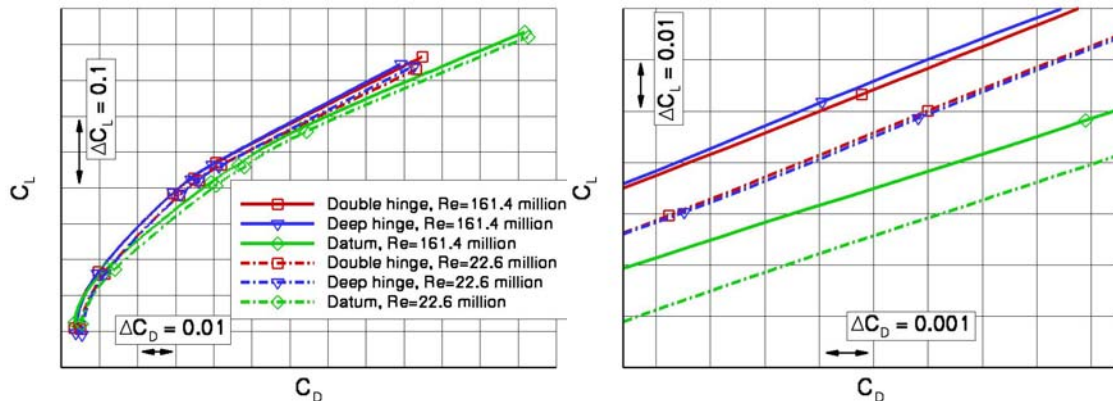
Figure 8 Influence of Reynolds number on predicted drag polar, M=0.25; a) Left: full computed range; b) Right: detailed view around design lift coefficient, showing configuration dependent Reynolds number impact.

7   Integration of CFD and experiment

The benefits of interactively discussing the results of CFD and experiment are outlined. After the wind tunnel test, initial comparisons of predicted data with the raw experimental data showed gaps. In view of the CFD-code acceptance test, the differences were believed to be unrealistic and effort was devoted to resolve this issue. Since the balance is situated below the wind tunnel floor, taking the pylons and struts into account in the CFD-analysis is a natural way of obtaining the impact of the model supports on the force data. At NLR, the pylons and the parts of the struts that are exposed to the flow have been included in the computational mesh of the double-hinge configuration. As a result, the mesh increased in size to 6.6 million cells. No exact match in exposed strut length is possible, since in the wind tunnel the front strut is used for incidence control. However, sufficient strut lengths are used to obtain a reliable impact on the flow around the configuration. An impression of the geometry included in the computational mesh is shown in Figure 9a. Comparisons have been made between results for the double-hinge configuration with and without the pylons and struts. Since CFD-methods allow for computing forces on selected parts of the geometry, the impact of the pylons and struts has been visualised separately. It should be kept in mind, however, that data for the configuration with pylon are extracted from the flow fields including the struts. In Figure 9b, the lift curves show that the addition of pylons and struts result in slightly lower lift values. The addition of pylons to the wing leads to a small increase in drag (Figure 9c), while the addition of the exposed parts of the struts contributes significantly to the drag. A drag increase in the order of 60-80 drag counts is found over the computed range. For the pitching moment, the addition of pylons shifts the curve to less negative values, while addition of the struts counteracts this effect (Figure 9d). Only at

the higher range of lift values there is a deviation from the double-hinge configuration without pylons and struts.

The indications for the drag due to struts have led to a critical review of the correction procedure for experimental forces and moments. As indicated earlier, the current wind tunnel model support having the centreline strut in front of the wing struts has been used for the first time, and a verified wind tunnel data correction procedure could be established for this particular type of wind tunnel model support.
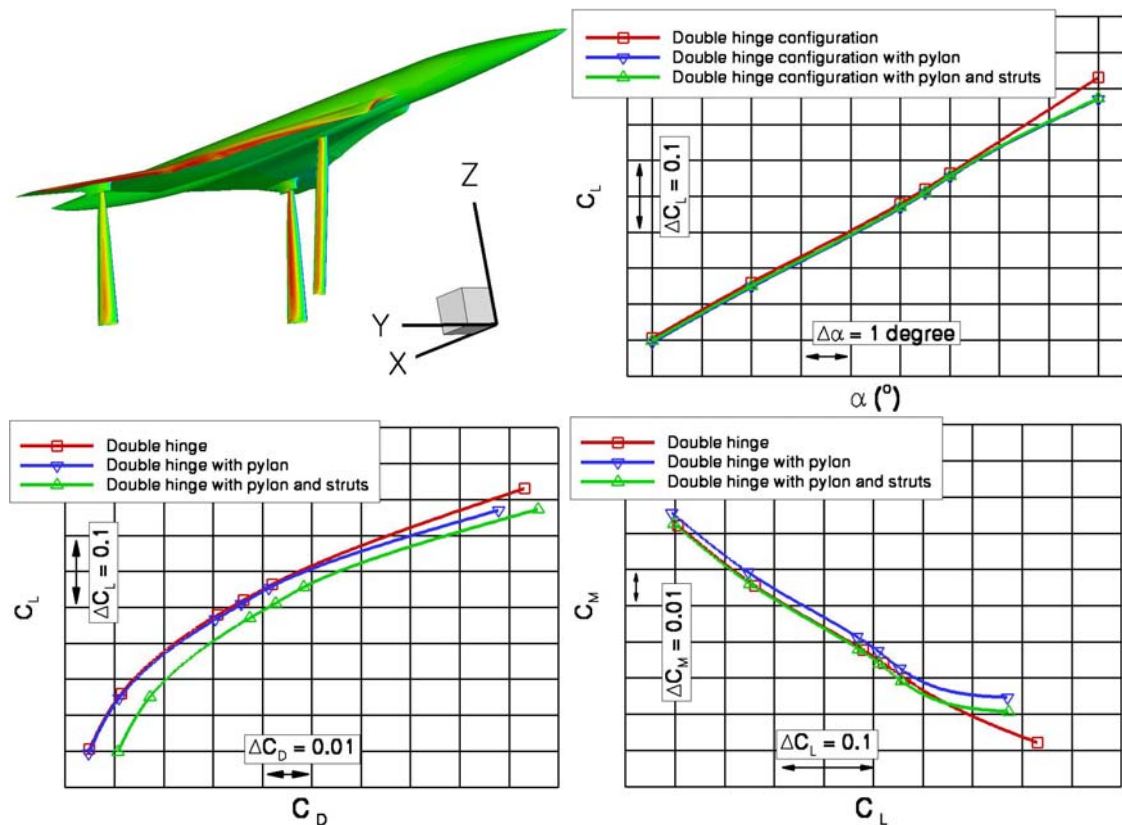
Figure 9 Results for double-hinge configuration with and without pylons and struts at M=0.25 and Re=22.6 million; a) Top left: impression of modelled geometry showing pressure distribution at design condition; b) Top right: lift curves; c) Bottom left: drag polar; d) Bottom right: pitching moment curves.

In Figure 10, a comparison of computed and experimental pressure distributions is shown for the double-hinge configuration (left) and the deep-hinge configuration (right) at design lift. For the double-hinge configuration, results including the pylons and struts are also depicted. It is shown that the impact of the pylons and struts on the pressure distribution is limited to local effects, as is shown on the lower side of the section at 61 percent of semi-span where the inclusion of pylons and struts leads to a closer match with experimental data. Overall, the predicted pressure distributions are acceptably close to the experiment. For higher lift values exhibiting larger regions of separated flow, the differences in computed and measured pressure

data are usually somewhat larger. Furthermore, the innovative devices show mainly attached flow at the design condition, in contrast to the datum configuration, see e.g. [5].
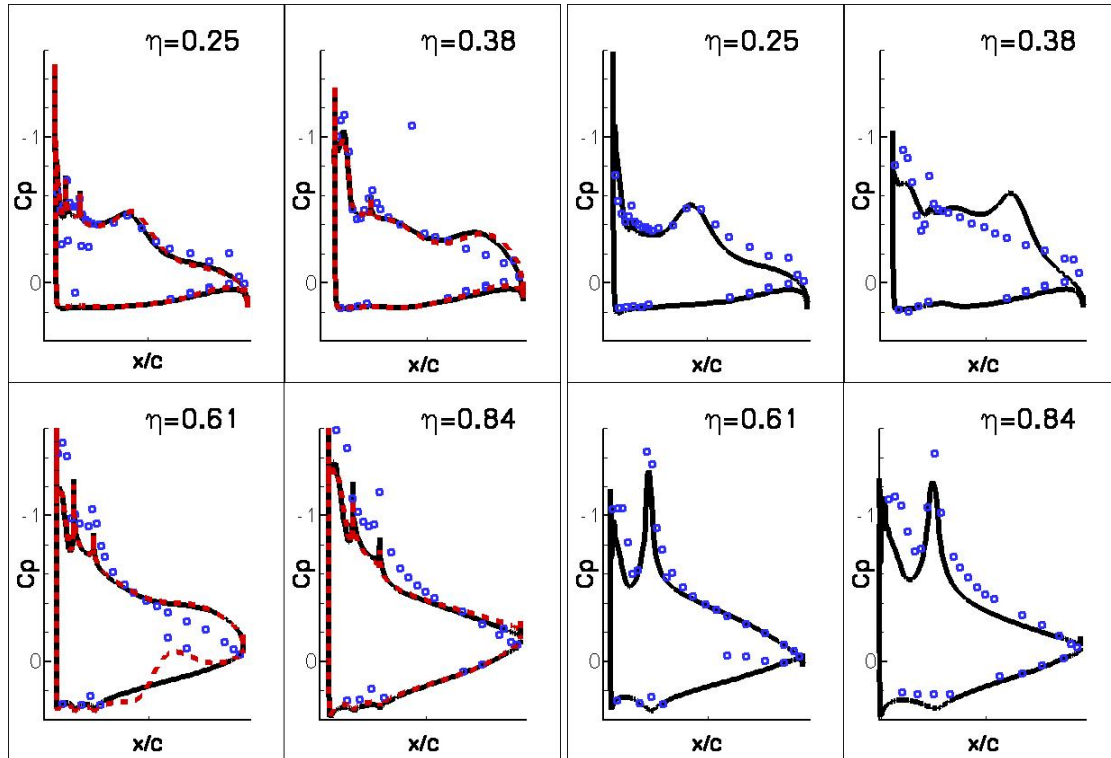
Figure 10 Comparison of computed (black lines) and experimental (blue symbols) pressure data at design lift, M=0.25, Re=22.6 million; Left: double-hinge configuration, red lines indicating results including struts; Right: deep-hinge configuration.

Finally, the comparison with experimental force data for each of the three configurations is shown in Figure 11. For the datum configuration, the computed drag polar is rather close to the experimental data, which is in agreement with previous experience using the data at lower Reynolds number from DNW-HST, see e.g. [5]. The drag is slightly higher than the experimental values, which can be explained by the usual drag dependency on mesh density, see also [5]. From this rather good comparison, a slightly disappointing comparison emerged for both innovative devices. Although correct at low lift coefficients, the computed values tend to drift away from the experimental data at higher lift coefficients. To date, no fully satisfactory explanation has been found to account for these differences. Erroneous prediction of the progressive development of separated flow over the new leading-edge devices could be part of the explanation. New indications about subtle but non-negligible wind tunnel interference effects on vorticity distribution and eventually vortex breakdown are also emerging see e.g. [9]. A more detailed study in this field is recommended.

Despite the differences in computed and measured values, the trends are correctly represented in the computational results. It is found that predicted differences – small as they are - between

double-hinge and deep-hinge configuration are confirmed by experiment, showing a slight advantage of the double-hinge design at wind tunnel model scale Reynolds number.
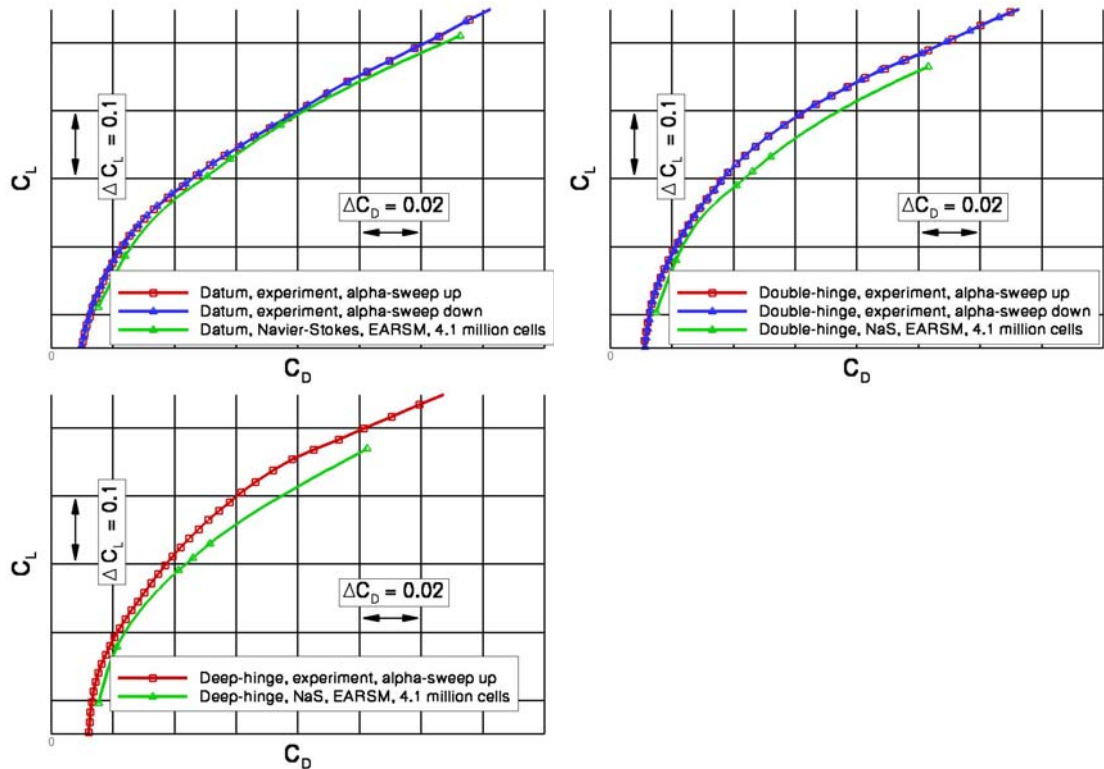
Figure 11 Comparison of computed and final experimental balance force data for each configuration at M=0.25 and Re=22.6 million; Top left: datum configuration; Top right: double-hinge configuration; Bottom: deep-hinge configuration.

8 Impact of geometrical changes

Another issue that needs to be addressed is related to performance differences encountered between the evolution phase of the double-hinge configuration and the final analysis phase including wind tunnel tests. Since identical meshes and the same flow solver have been used, the only plausible explanation has to be found in geometrical differences. In the evolution phase, the configuration has been modelled using an infinite fuselage to resemble the sting-mounted wing-body configuration as used in previous wind tunnel tests (see Figure 4). In the analysis phase, the wind tunnel model as shown in Figure 5 has been modelled, employing a finite fuselage. Further geometrical differences are found in the application of wing tip rounding in the planform. Figure 12 illustrates the geometrical differences.

From computational results, it has been found that the contribution of the fuselage to the total drag is nearly indifferent to the type of fuselage used. In this comparison, the forces on the

infinite fuselage are taken into account up to the point where the sting actually begins, in accordance with the wind tunnel model in Figure 4. The main differences in contributions to the total drag are found on the wing. Geometrical differences on the wing include the wing tip rounding, and the slightly altered wing-body intersection due to the finite fuselage. Part of the double-hinge flap system is cut away by rounding the wing tip. From comparisons of local force data, no significant changes close to the wing root are observed, see Figure 13. At the wing tip, a significant change is found in local coefficients. Apparently, the tip vortex has moved to a position further inboard due to the wing tip rounding. The tip vortex is also suspected to become stronger, since part of the beneficial leading-edge flap system is cut away by the wing tip rounding thus giving separation and vortical flow development at an earlier stage. Locally, higher lift and drag values are found, as well as visible influences in the distribution along the span. The comparisons shown in Figure 13 indicate that more care is required in establishing the final geometrical finishing touch of the configuration.
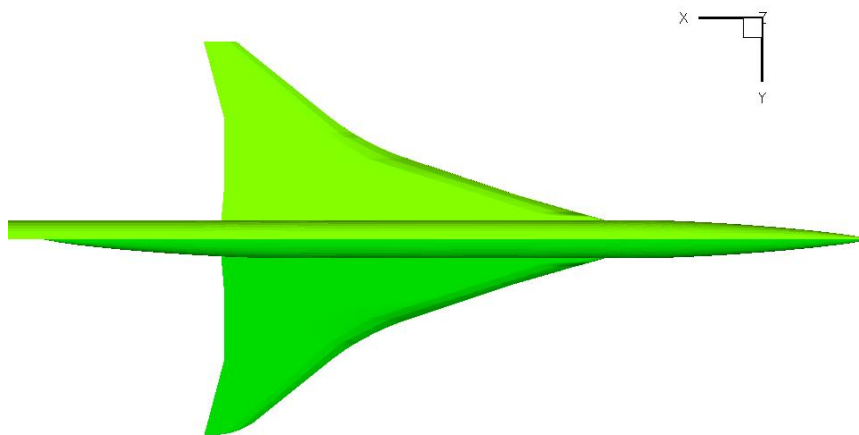
Figure 12 Geometrical differences during design phase (top half, straight wing tip, infinite fuselage) and validation phase (lower half, rounded wing tip, finite fuselage, slightly changed wing-body intersection).
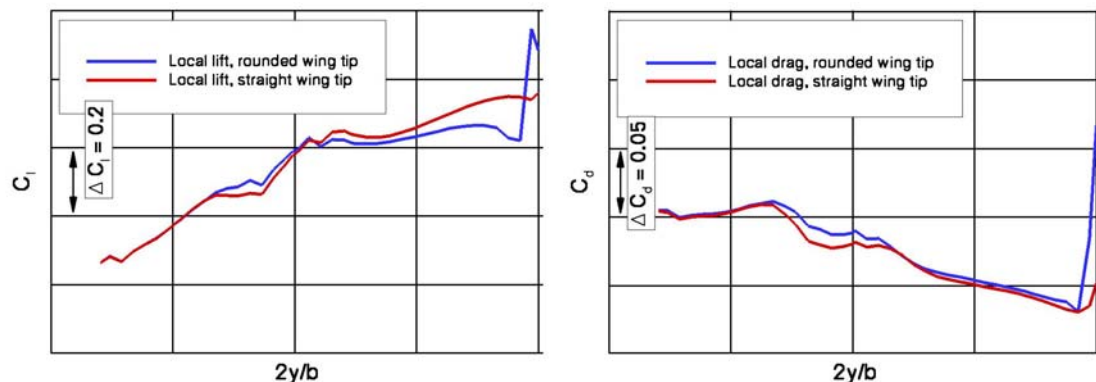
Figure 13 Comparison of local lift and drag coefficients along the wing span for straight and rounded wing tip at approximately design lift condition

9   Conclusions

Analysis and improvement of the low-speed aerodynamic characteristics of a supersonic civil transport aircraft using different types of leading-edge devices has been conducted. As is common in current configuration development, the usage of CFD-computations is widely accepted for wings with attached flow. For the types of wings under consideration, involving large regions of separated flow, validation of the CFD-method has been conducted using wind tunnel data obtained for a 1/80 scale model. Subsequently, the CFD-method has been used in leading-edge device evolution studies, and selection of promising devices is based on CFD-results. Validation of the promising leading-edge flap systems has been conducted by experimental investigation, using a 1/22 scale wind tunnel model. The mounting of the wind tunnel model has raised questions about its impact on measured aerodynamic coefficients. The role of CFD proved to be crucial in terms of separating the specific influences of the applied struts and the pylons that are used to attach the struts to the comparatively thin wing. The interaction between CFD-analysis and experimental data assessment proved to be beneficial in the determination of the final wind tunnel data correction procedure for strut interference, and in gaining understanding of the development of the flow field with and without struts. Furthermore, CFD has shown its merits in assessing influences of geometrical differences. Thus, it is found that knuckle rounding at the hinge lines is showing benefits in the Reynolds number extrapolation, whereas wing tip rounding is reducing the anticipated aerodynamic efficiency. Trends in different leading-edge flap systems are correctly predicted with CFD. Despite the presence of significant regions of separated flow, typical for this type of configurations, the use of Navier-Stokes methods employing state-of-the-art turbulence models is shown to have a major impact on the success of configuration development.

10 Acknowledgements

11 References

1. D.A. Lovell. *European Research to Reduce Drag for Supersonic Transport Aircraft.* AIAA-99-3100, 1999.

2. J. van Muijden and A. Elsenaar. *Transonic Aerodynamic Efficiency Assessment of an Optimised Supersonic Civil Transport Using CFD.* Proceedings of ECCOMAS Conference, Barcelona, 11-14 September 2000, also NLR-TP-2000-373, 2000.

3. U. Herrmann. *High Performance High-Lift System Design for SCT in the EC-Project EPISTLE.* Proceedings of ECCOMAS Conference, Finland, July 2004.

4. G.E. Erickson and H.A. Gonzalez. *Pressure-Sensitive Paint Investigation of Double-Delta Wing Vortex Flow Manipulation.* AIAA 2005-1059, 2005.

5. J. van Muijden and A. Elsenaar. *Numerical Prediction Capabilities and Analysis of Flow Development for a Supersonic Civil Transport at Low Speed.* Proceedings of CEAS Aerospace Aerodynamics Conference, Cambridge, 10-12 June 2002, also NLR-TP-2002-496, 2002.

6. J.C. Kok, J.W. Boerstoel, A. Kassies and S.P. Spekreijse. *A Robust Multi-Block Navier-Stokes Flow Solver for Industrial Applications.* Proceedings of ECCOMAS Conference, Paris, 1996, also NLR-TP-96323, 1996.

7. H.S. Dol, J.C. Kok and B. Oskam. *Turbulence Modelling for Leading-Edge Vortex Flows.* AIAA-2002-0843, January 2002.

8. U. Herrmann, A. Press, C.M. Newbold, P. Kaurinkoski, C. Artiles, J. van Muijden and G. Carrier. *Validation of European CFD Codes for SCT Low-Speed High-Lift Computations.* AIAA-2001-2405, June 2001.

9. M.R. Allan, K.J. Badcock, G.N. Barakos and B.E. Richards. *Wind Tunnel Interference Effects on Delta Wing Aerodynamics – Computational Fluid Dynamics Investigation.* Journal of Aircraft Vol. 42, No. 1. January-February 2005.